Radial Dependence of Axial Load Cells

Alex Nathan Kahn

Independent Study (ME 497 JWP)

Instructor: Professor Emeritus James W. Phillips

12/15/2014

Background

Various industrial practices use load cells to determine compressive axial forces. Typical axial load cells contain surface-mounted strain gages that measure electrically the elastic strain of a metallic cylindrical section under compressive stress. A load cell can respond linearly to an applied compressive load if its strain gages are arranged in a Wheatstone bridge. Multiplying a load cell's output voltage by a constant value determines the load applied to the cell. While a linear relationship is convenient, it may be valid only under ideal conditions. Asymmetric loading geometry can significantly impact localized strain in a load cell. Since strain gages respond linearly to localized strain, asymmetric loading may cause a nonlinear response to applied load. The relationship between loading conditions and output variation is crucial to industrial load cell accuracy.

Mechanics

This investigation concerns the use of a specially manufactured 6061-T6 aluminum axial load cell. The load cell contains two pairs of diametrically opposed strain gage rosettes. One pair is surface-mounted, corresponding to conventional load cell design. The other pair is mounted in a recessed slot such that rosettes are mounted on the neutral surface of the load cell wall. The neutral surface is located halfway between the inner and outer load cell wall surfaces. Figure 1 depicts the general load cell geometry and the position of a slot rosette. Figure 2 details the relative positions of a body rosette and a slot rosette on opposite sides of an electrical terminal array.

Each rosette contains an axial strain gage element and a transverse strain element. Strain gage elements from each pair of rosettes comprise the resistors of two separate Wheatstone bridges; there is a slot Wheatstone bridge and a body Wheatstone bridge. Figure 3 illustrates the circuit scheme used for both Wheatstone bridges. Terminals P+, P–, S+, and S– correspond to the positive and negative power and signal nodes, respectively. Table 1 provides the connector pin scheme for the connectors used in the present study. The strain gages have the same nominal resistance. For sufficiently small changes in resistance, the normalized output voltage of each Wheatstone bridge is given by [1]

$$\frac{\Delta E}{V_0} = \frac{1}{4}\left(\frac{\Delta R_1}{R_1} - \frac{\Delta R_2}{R_2} + \frac{\Delta R_3}{R_3} - \frac{\Delta R_4}{R_4} \right), \tag{1}$$

where

ΔE is signal voltage

V_0 is power voltage.

For each strain gage,

$$\frac{\Delta R}{R} = S_g \varepsilon, \tag{2}$$

where

ε is localized strain

S_g is the strain gage factor.

For uniaxial stress loading, it follows that normalized output voltage is linearly related to applied compressive load under ideal axial loading conditions:

$$\frac{\Delta E}{V_0} = \frac{S_g(1+\upsilon)}{2AE}P, \tag{3}$$

where

υ is Poisson's ratio

A is the cross-sectional area of the load cell wall

E is the elastic modulus of the load cell material

P is the applied compressive load

S_g is the strain gage factor.

Ideal versus actual response

A linear relationship between applied compressive load and normalized output voltage may be valid only under ideal loading conditions. In the case of axial load cells, ideal loading conditions imply constant axial stress throughout the region in which a compressive load is transmitted. Loading must be symmetric about a load cell's neutral surface for constant axial stress to occur. The load cell used in this study is treated as a thin-walled cylindrical shell. The neutral surface of a thin-walled cylindrical shell is located halfway between the inner and outer wall surfaces. Figure 4 displays asymmetric loading about a load cell's neutral surface. Deviation from symmetric loading about a load cell's neutral surface will impose a tangential end bending moment in addition to an applied compressive load. A tangential bending moment can be conceptualized as the turning action applied to a tube sock as the sock's open end is rolled down.

Bending moments can significantly alter the state of localized strain throughout a load cell [2]. Bending moments can impose large strain deviations in the vicinity of a conventionally mounted body strain gage. It follows that nonideal loading conditions may cause divergent linear output responses. However, the neutral surface may be exempt from bending moment strain deviations. The load cell used for this investigation contains body-mounted and slot-mounted strain gages. Both mounting styles are incorporated in an effort to determine deviations between body measurements and neutral surface measurements.

Experimental procedure

Initial testing was performed with the aid of a 200-kip Riehle universal testing machine and 2 Vishay Instruments P-3500 strain indicators. The strain indicators were connected to the load cell by the cell's Wheatstone bridge connector pins. The strain indicators provided voltage V_0 across P+ and P– in each of the cell's Wheatstone bridges. The strain indicators also measured voltage across S+ and S–. As is typical in many load cell applications in which a strain indicator is employed for output measurement, a representative gage factor value was assumed for the load cell [1]. In this case, a value of 2 was used for the gage factor. The strain indicators displayed strain values in units of microstrain. Indicated strain values were recorded by hand and then entered into a computer. The strain values were divided by 2000 to convert to normalized output voltage in mV/V [1].

A circular plate was placed in between the load cell and the loading platens of the universal testing machine during initial testing. It is assumed that the load cell had not sustained any significant compressive loading before initial testing.

Initial results

Table 2 presents data from initial testing. The slot output was noticeably larger than the body output. Also, while the slot output was approximately linear, the body output was nonlinear. Thus, the initial testing indicated that the load cell's neutral surface may be negligibly affected by loading geometry. In addition, the geometry of loading may impose significant deviations from linearity in body mounted strain gage measurements.

In view of the results of initial testing, it was determined that a more controlled end loading method would be required in order to characterize the response of the load cell to varying end conditions.

Acrylic radial variance rings

Four sets of loading contact rings were manufactured to impose multiple radial loading conditions. An Epilog Fusion laser cutter cut the rings from 0.125 inch-thick acrylic plastic. Figure 5 depicts the four sets of rings. From left to right the sets of rings are referred to as inner, neutral, outer, and whole, respectively.

The inner ring, outer ring, and whole ring are concentric with respect to the load cell axis, but are asymmetric with respect to the neutral surface of the load cell wall. The rings are designed with neutral surface asymmetry to impose tangential bending moments on the ends of the load cell. As an example, Figure 6 details the placement of an outer edge ring. Figures 7 through 9 illustrate dimensions for the inner ring, outer ring, and whole ring, respectively. The inner rings rest on the inner edge of the load cell. The outer rings rest on the outer edge of the load cell. The whole rings rest across the whole face of the load cell, in accordance with conventional loading geometry.

The neutral ring is symmetric about the neutral surface of the load cell wall. The neutral ring is designed with neutral surface symmetry to avoid the generation of a tangential bending moment at each end of the load cell. Figure 10 provides neutral ring dimensions. The neutral rings rest on the neutral surface of the load cell wall during loading.

Acrylic ring results

Initial testing procedures were repeated with acrylic rings. Figure 11 is a photograph of the load cell inside the universal testing machine during testing. Rings were placed above and below the load cell at points of contact with the universal testing machine. Table 3 details acrylic ring testing configurations. Acrylic rings deformed plastically during testing. Test #4 combined ring types because an outer ring fractured during test #3. After plastic deformation was observed, the rings were abandoned because of their insufficient strength. However, data were still gathered during testing.

Figure 12 displays acrylic ring testing data. Test numbers correspond to the configurations detailed in Table 3. At 100 kips, the normalized body output voltage was about 25% less than the normalized slot output voltage during every test. Output also varied with loading geometry. At 100 kips, body and slot output values varied by at least 20% between

neutral and outer ring loading conditions. Thus, the radial variance in loading conditions had a significant impact on the load cell's output.

Metal rings

An Inventables milling machine cut metal rings from a sheet of 6061-T6 aluminum, according to the dimensions in Figures 7 through 10. Figure 13 is photograph of the metal rings with the load cell used in this study. Initial metal ring data were gathered by hand according to acrylic ring testing procedures. Ultimately, Vishay Instruments 5100B scanners and StrainSmart 5000 software were used to acquire digital data. The scanners were connected to the pins labeled "DAQ connector" in Figure 13, then the load cell was cyclically loaded and unloaded between 0 and 50 kips for each ring type. Applied load and normalized output voltage data were then exported in American Standard Code for Information Interchange (ASCII) text format.

Metal ring results

Normalized output voltage was plotted versus compressive load for each ring configuration. The curves were separated into loading cycles, and the final cycle for each ring configuration was determined. See Figure 14.

At 50 kips the normalized output voltage varied between 0.82 and 1.36 mV/V, depending on which ring configuration was used and which strain gage bridge was monitored. In addition, the load cell response was nonlinear between 0 and 20 kips. The slot output was consistently higher than the body output. Outer edge loading condition curves varied depending on whether a compressive load was applied up to 50 kips, or unloaded to 0 kips. Outer edge loading direction variation is displayed by the loops in the outer edge curves. Outer edge loading condition curves had a consistently smaller slope than all other curves. Body and slot gage responses varied with loading conditions. Thus, neutral surface strain gage placement may not counter the effects of variable radial loading conditions. As seen in Figure 14, dramatic variance in load cell response can occur as a result of radial loading variance.

Additional theoretical considerations

Roark's formulas [2] provide equations for theoretical analysis of thin-walled cylindrical shells. The bending moment experienced by the load cell from this study can be theoretically calculated at various axial positions by considering a 4-inch-long cylindrical shell with dimensions similar to the cell. Applied tangential end bending moments will result in a changing internal bending moment along the axis of the load cell.

Figure 15 is a plot of internal bending moment versus axial position along the load cell. The bending moment approaches zero at the center of the load cell axis, but the bending moment is noticeably negative. The nonzero bending moment at the middle of the load cell may cause the cell response to vary with loading conditions, since the strain in the vicinity of the strain rosettes is partially determined by the bending moments incurred through radial loading variance.

There are significant theoretical complexities involved in calculating the end moments applied to the load cell. As depicted in Figure 1, the top and bottom edges of the load cell are not consistent with the thin-walled cylindrical shell geometry assumed in theoretical calculations. Although the exact end bending moments applied to the cell are unknown, loading conditions

that were asymmetric about the load cell's neutral surface clearly caused significant variance in the cell's response.

Conclusions

Although various experimental procedures were performed throughout this study, similar results were observed in each test. Load cell responses varied significantly with radial loading conditions, even if measurements were taken at the load cell's neutral surface. Variance was so dramatic that a normalized output voltage of 0.80 mV/V corresponded to a load between 28 and 49 kips, depending on loading conditions and which strain gage bridge was monitored. Significant measurement inaccuracies can be incurred through radial loading variance in axial load cells. In order to assure safety and efficiency, industrial businesses must be aware of the radial dependence of axial load cells.

Acknowledgements

I express my profound gratitude to Professor Emeritus James W. Phillips for his instruction throughout my independent study. He repeatedly offered me his knowledge about the various topics relevant to my endeavors, while regarding even the smallest details of my investigation. I delight in the attention Professor Phillips paid to my reports, especially his explanation of when to use a hyphen, n-dash, or an m-dash (-, –, or —). I am glad that I have had the opportunity to conduct my study under his supervision. Figure 16 is a photograph of Professor Phillips and me during metal ring testing.

I wish to thank several of the Talbot laboratory employees: Lee Booher, Steve Mathine, and Greg Milner. The attentive labor of these men allowed for me to continue my studies in a furnished laboratory setting.

Lastly, I wish to thank Joshua Kim. Josh guided me as I manufactured my metal rings which proved crucial to this study. I am grateful for his experience and helpfulness with regards to metallic milling.

References

[1] Phillips, James W. Strain Gages—Wheatstone Bridge. Notes for TAM 456, Experimental Stress Analysis. Accessed 2 September 2014.

[2] W.C. Young and R.G. Budynas. 2002. *Roark's Formulas for Stress and Strain*. McGraw-Hill.

Appendix

Table 1: Pin scheme.

Terminal	Male connector pin
P+	5
P–	7
S+	2
S–	4

Table 2: Initial testing data.

Applied compressive load	Body output	Slot output
kips	mV/V	mV/V
0	0.000	0.000
50	1.006	1.237
100	2.050	2.467

Table 3: Acrylic ring testing configurations.

Loading Conditions		
Test #	Top Ring	Bottom Ring
1	Neutral	Neutral
2	Neutral	Neutral
3	Outer	Outer
4	Whole	Outer

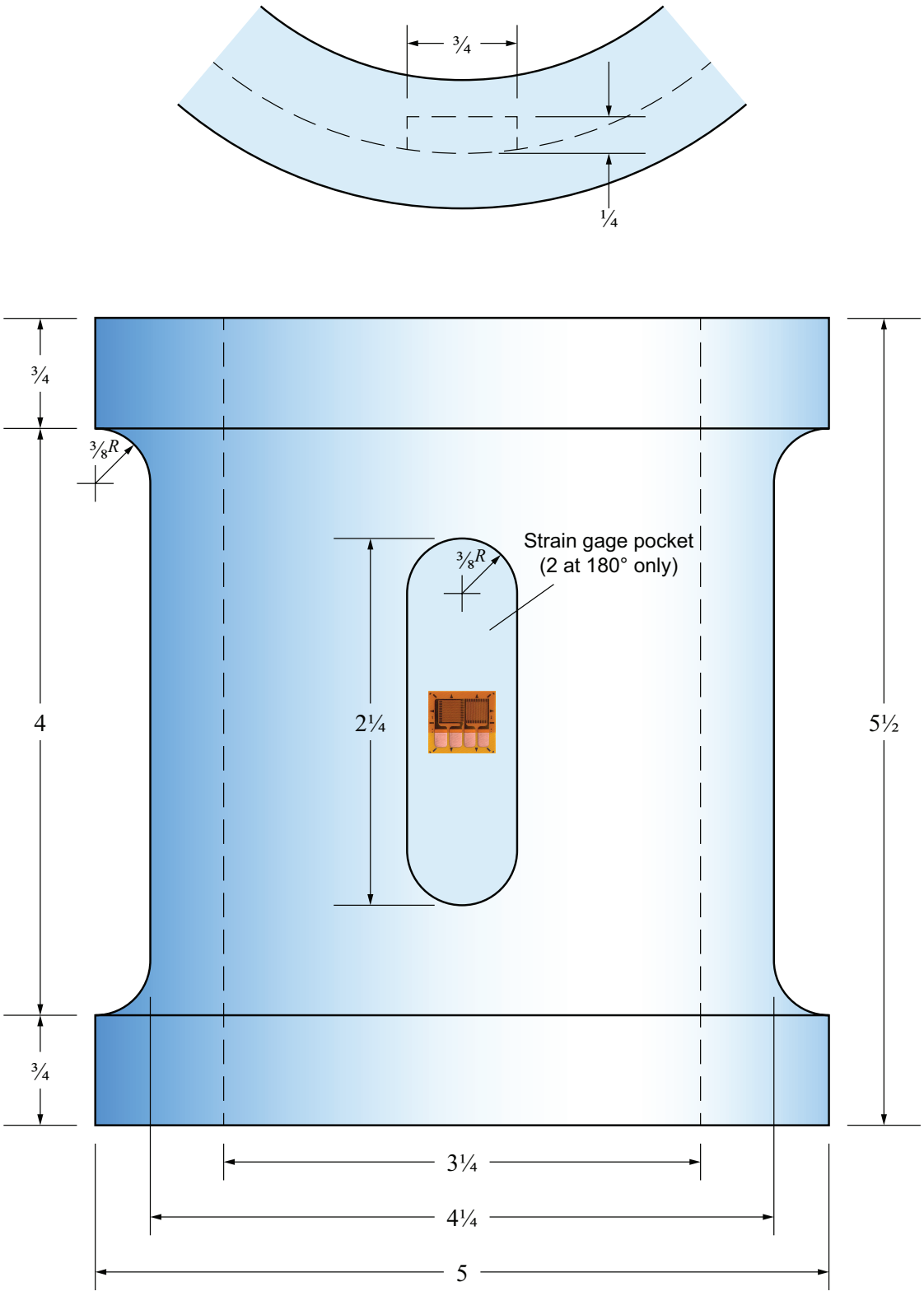

All values in inches.

Figure 1: General load cell geometry and slot rosette position.
(Drawing courtesy of Prof. James W. Phillips.)

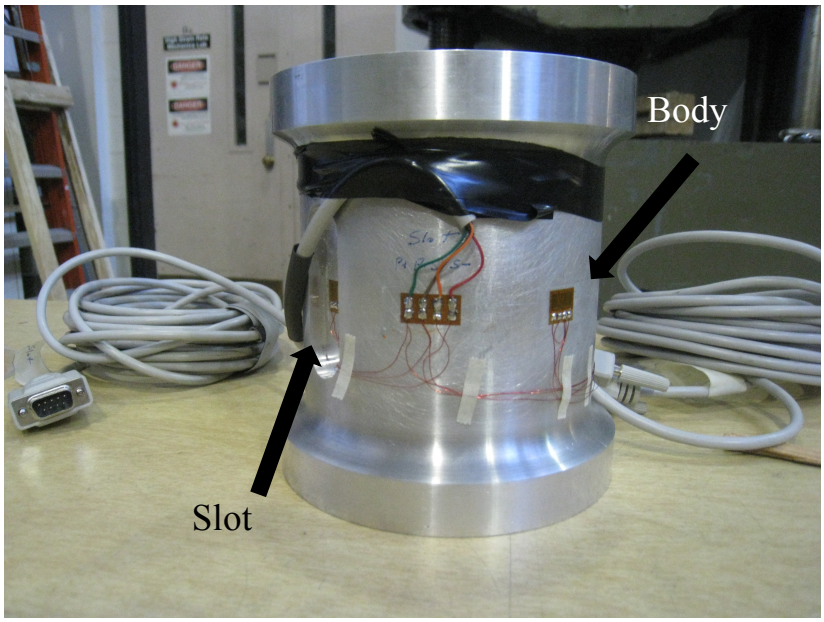

Figure 2: Body rosette and slot rosette position.

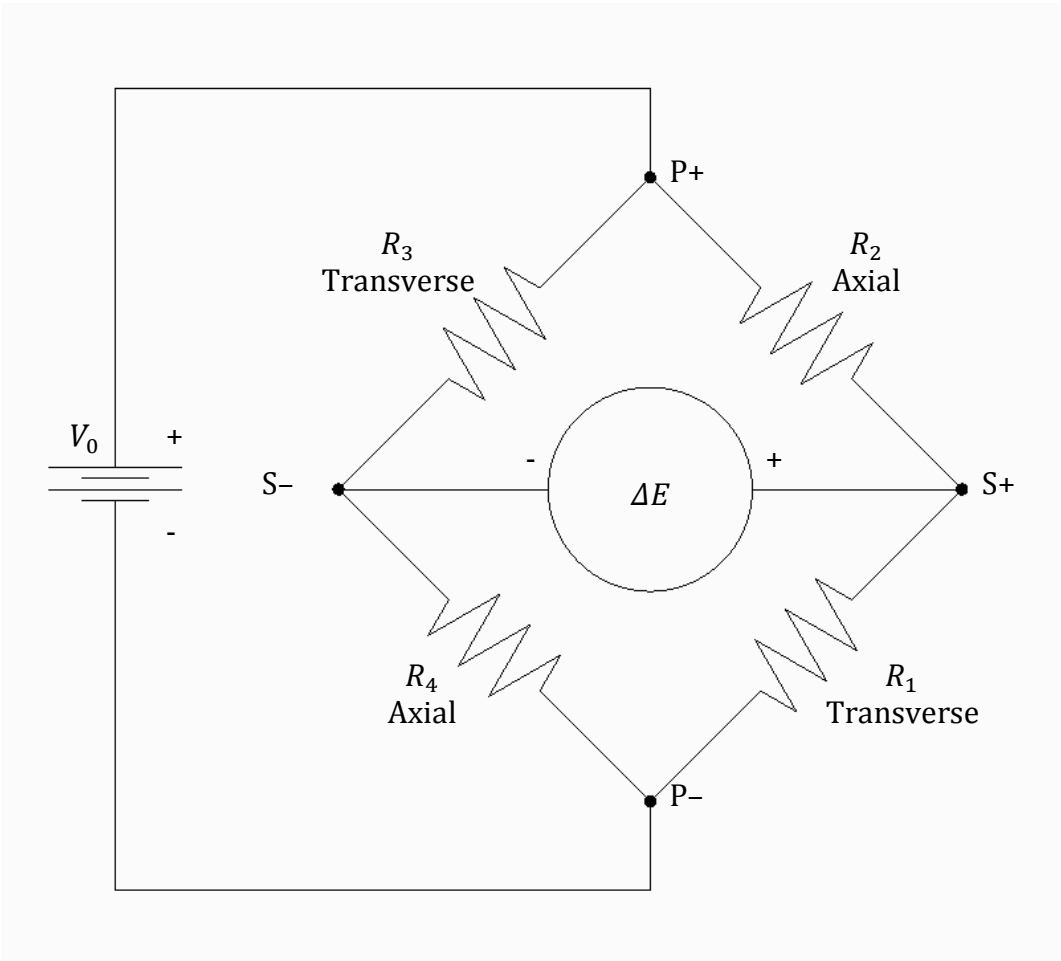

Figure 3: Rosette Wheatstone bridge.

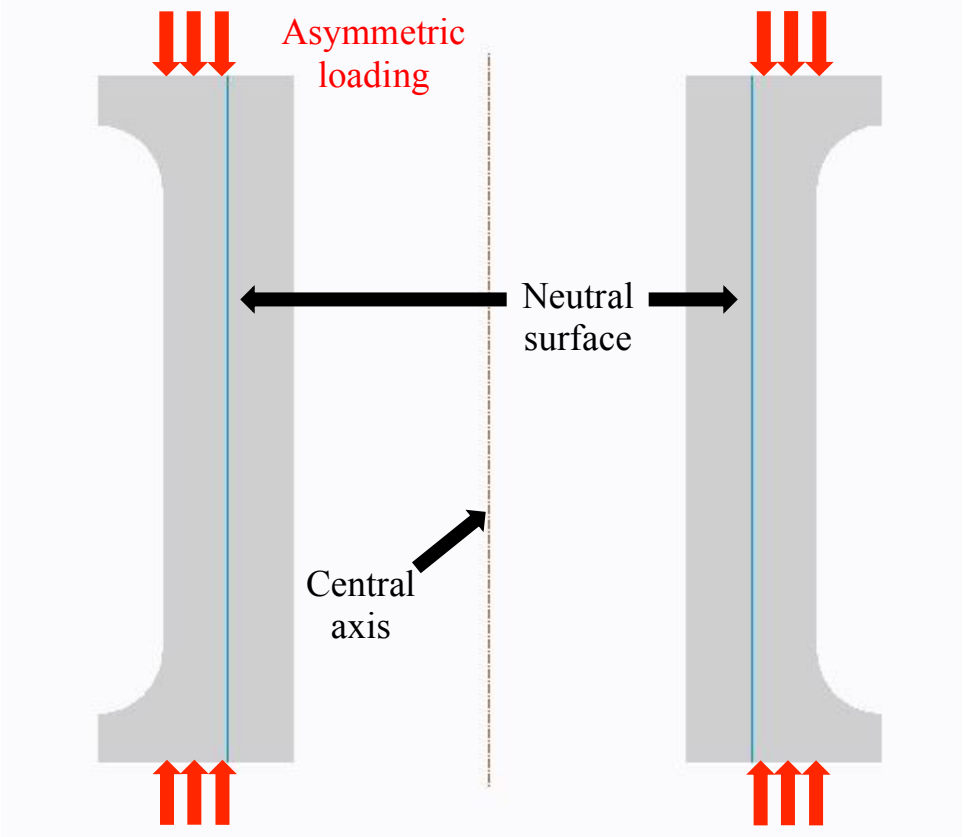

Figure 4: Neutral surface loading asymmetry.

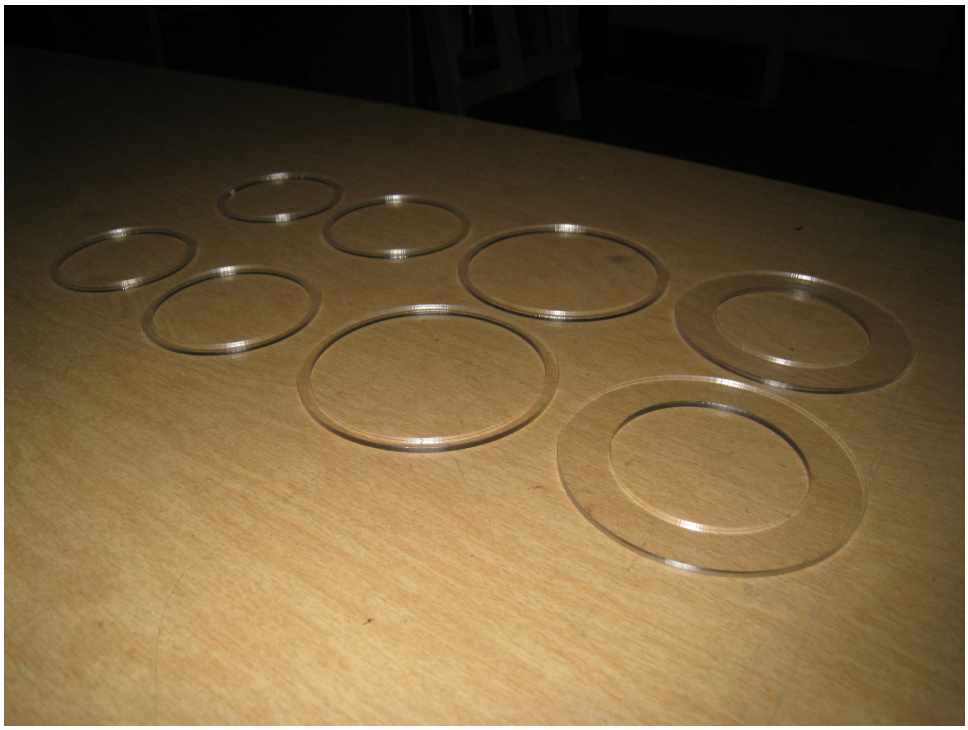

Figure 5: Acrylic loading rings.

Figure 6: Outer ring placement.

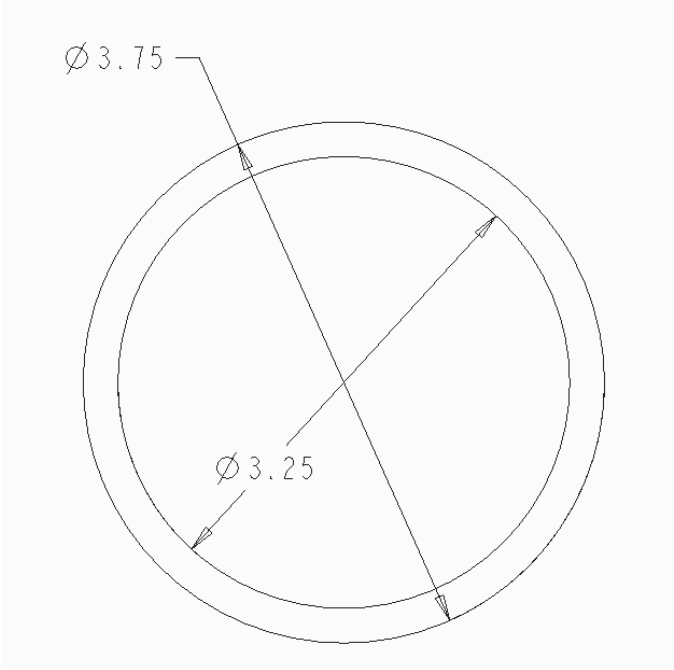

Figure 7: Inner ring dimensions in inches.

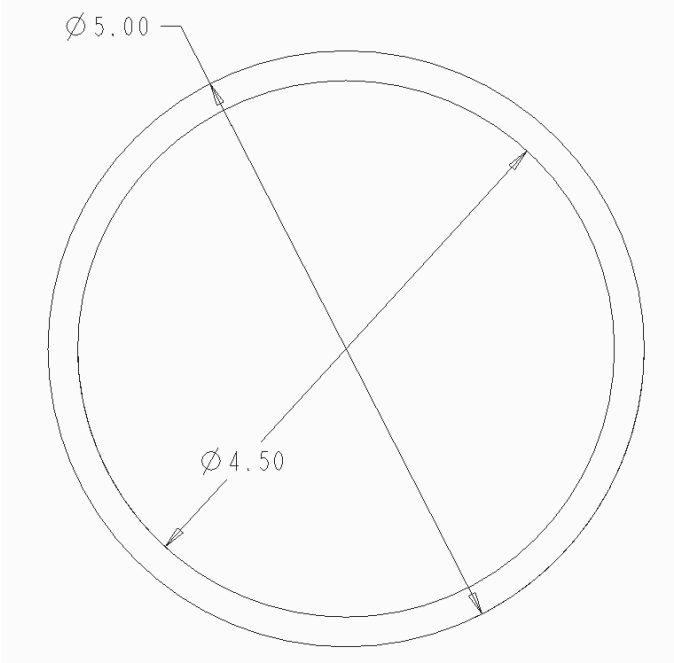

Figure 8: Outer ring dimensions in inches.

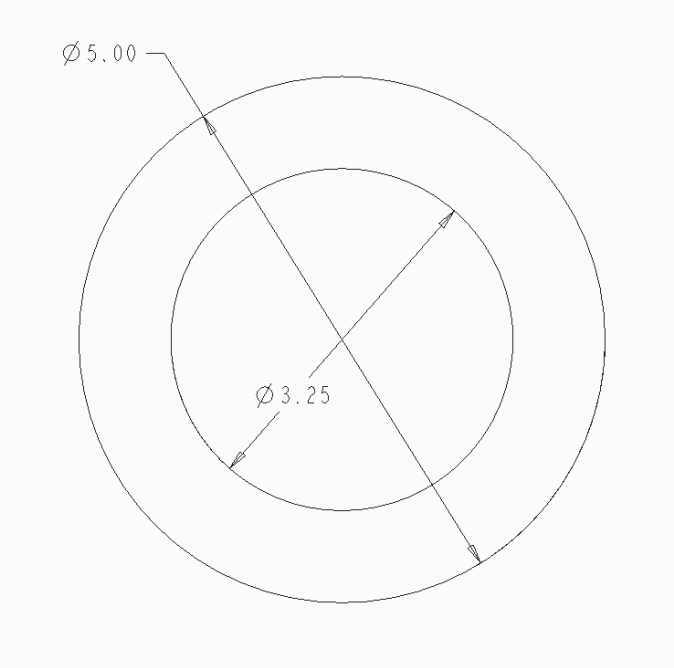

Figure 9: Whole ring dimensions in inches.

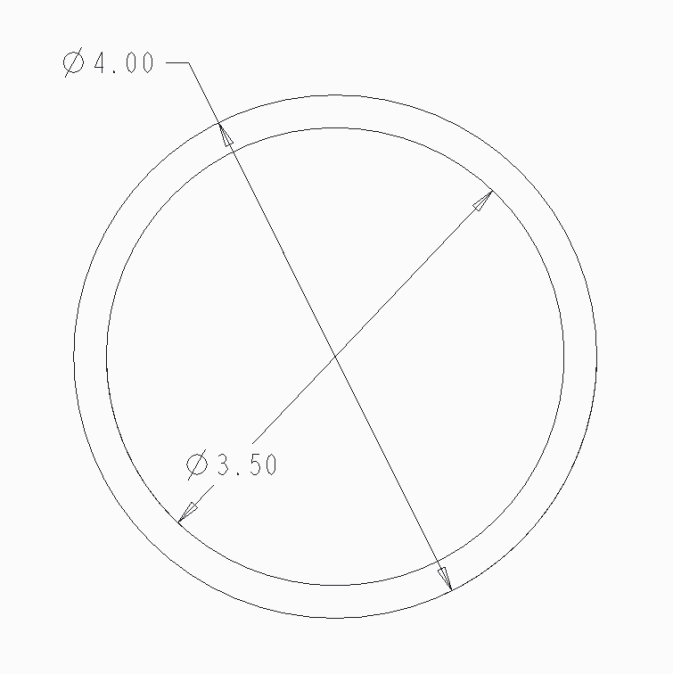

Figure 10: Neutral ring dimensions in inches.

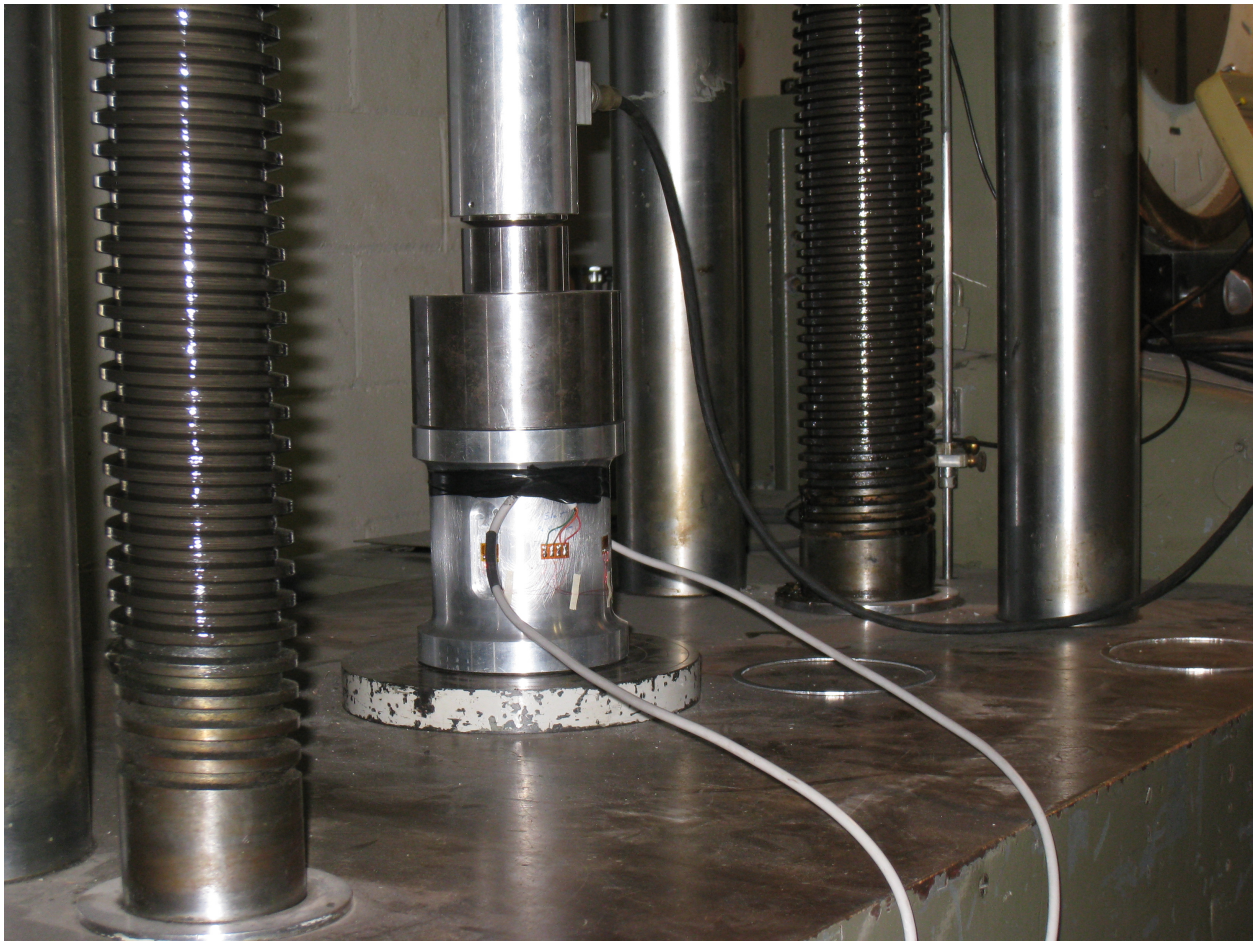

Figure 11: Load cell inside universal testing machine.

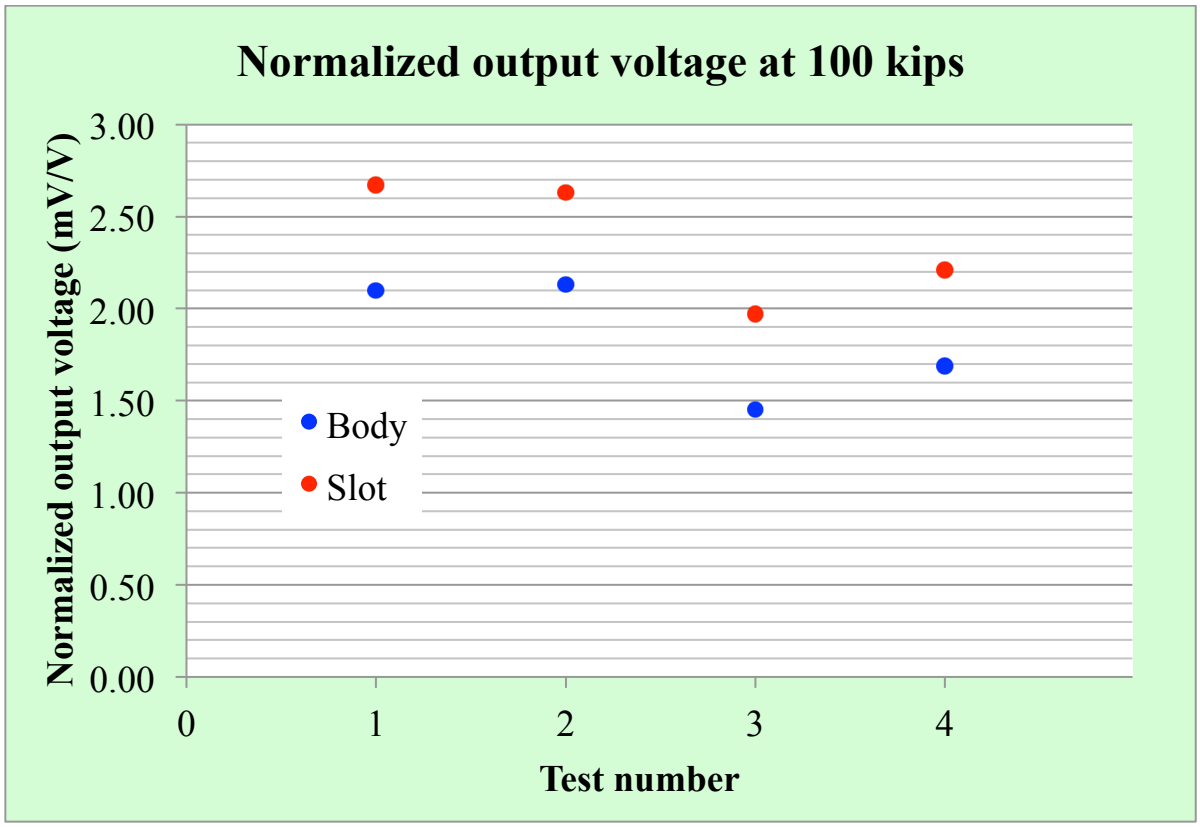

Figure 12: Acrylic ring testing data.

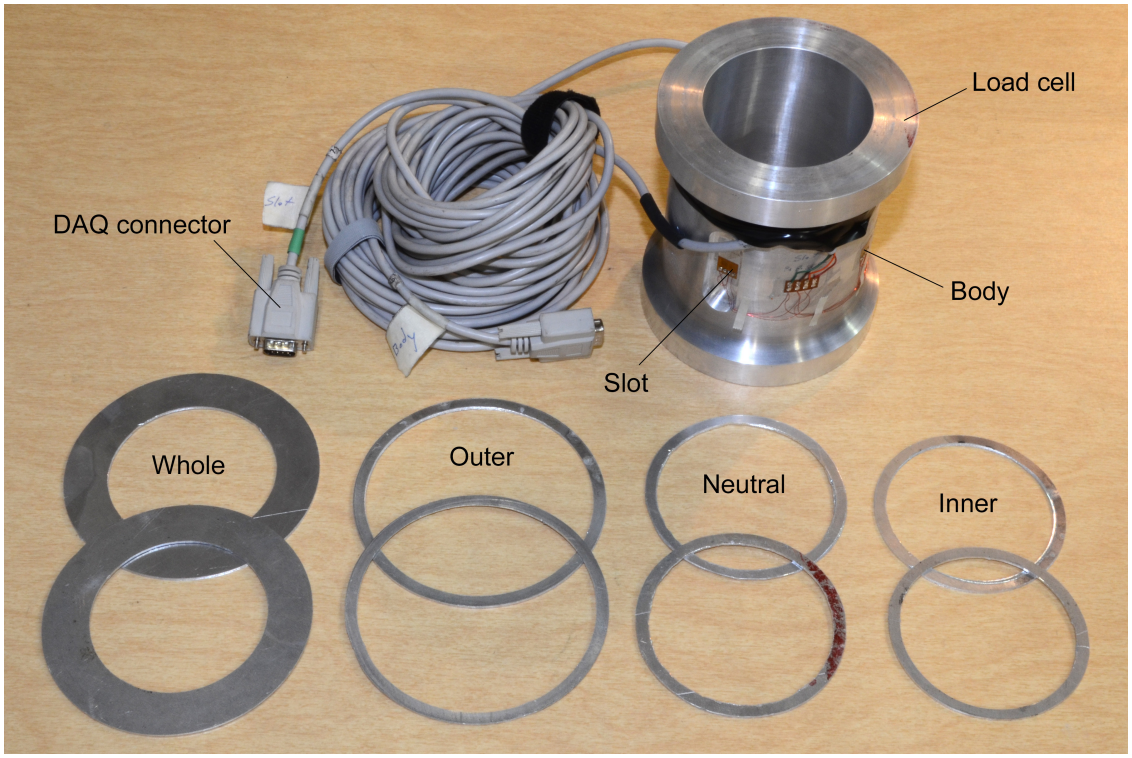

Figure 13: Load cell and metal rings.
(Photograph courtesy of Prof. James W. Phillips.)

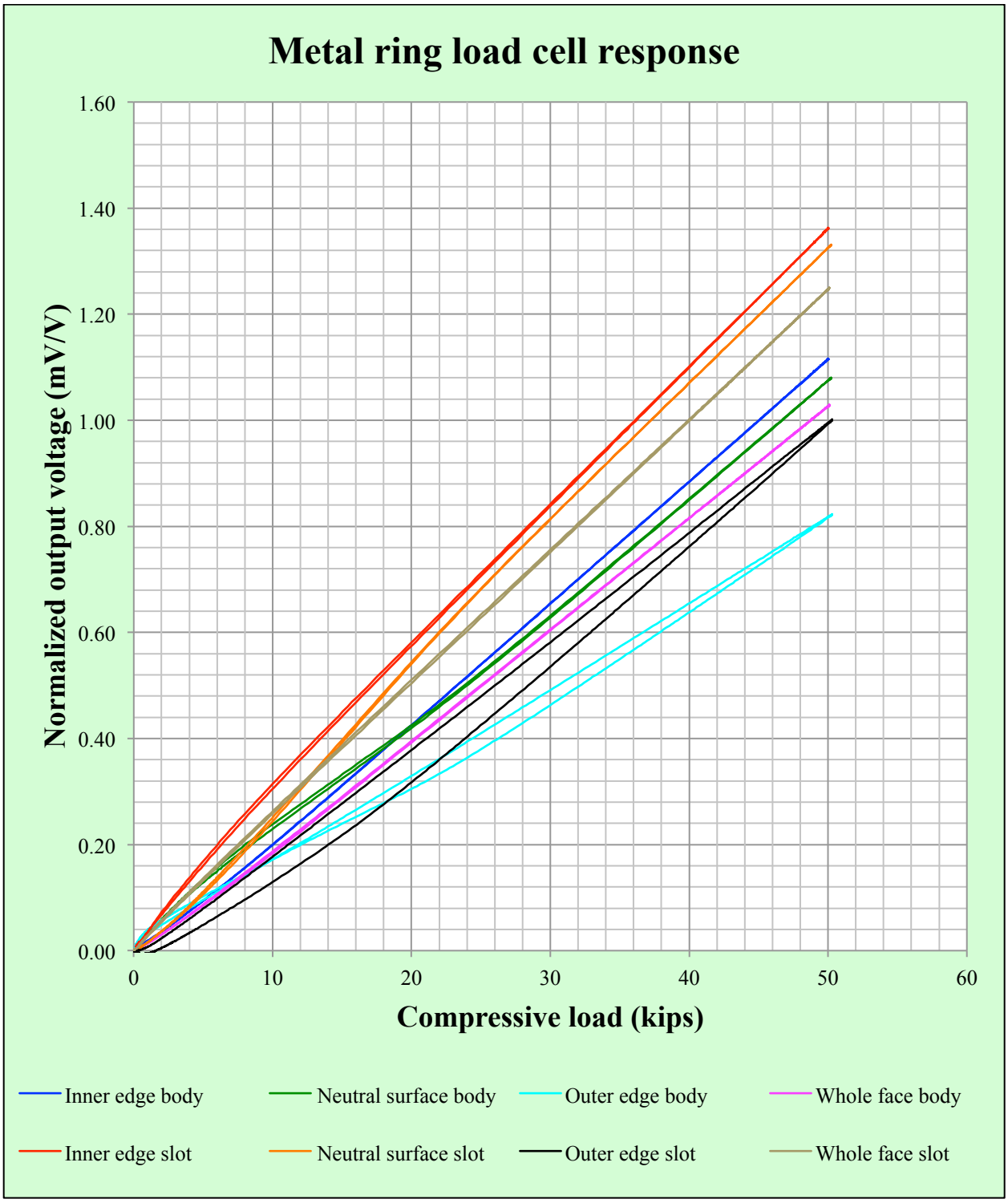

Figure 14: Metal ring load cell response.

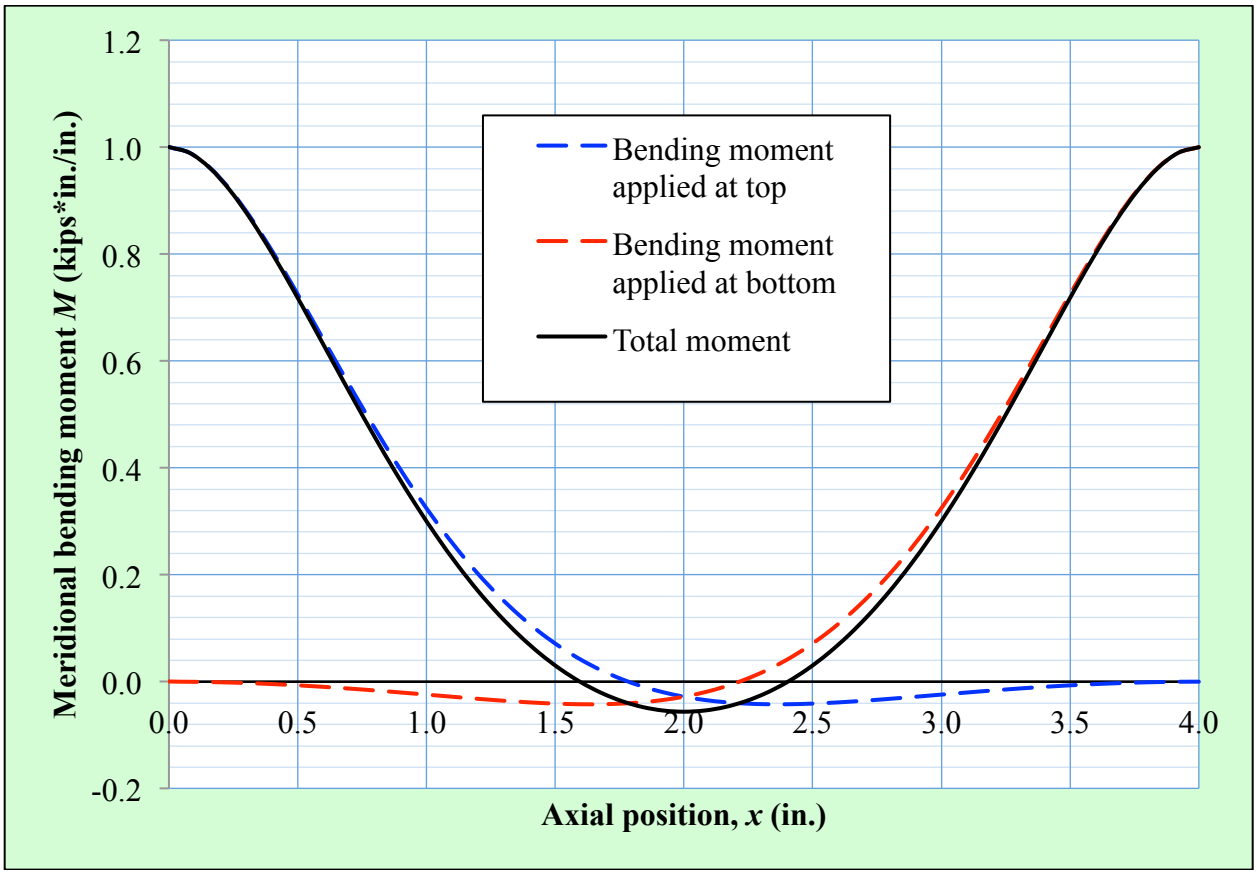

Figure 15: Theoretical load cell bending moment.
(Adapted from a spreadsheet provided by Prof. James W. Phillips.)

Figure 16: Metallic ring testing. From left to right: Alex Nathan Kahn, Professor Emeritus James W. Phillips.
(Photograph courtesy of Prof. James W. Phillips.)